FULL PAPER

Dalton
www.rsc.org/dalton

Synthesis, characterization and DFT studies of the cobalt(III) complex of a tetrapodal pentadentate N_4S donor ligand

Clint A. Sharrad,[a] Germán E. Cavigliasso,[b] Robert Stranger[b] and Lawrence R. Gahan*[a]

[a] *Chemistry Department, The University of Queensland, Brisbane, QLD 4072, Australia*

[b] *Department of Chemistry, Faculty of Science, Australian National University, ACT 0200, Australia*

Received 15th January 2004, Accepted 1st March 2004
First published as an Advance Article on the web 23rd March 2004

The synthesis of the pentadentate ligand 2,6-bis(3,3-dimethyl-2,4-dioxocyclohexanyl)-4-thiaheptane (N_4Samp) is described. The synthetic pathway involves the coupling of two 1,3-(dimethylenedioxy)-2-methyl-2-(methylene-*p*-toluenesulfonyl)propane moieties with sodium sulfide and subsequent synthetic elaboration to prepare the final N_4S donor system. The cobalt(III) complex $[Co(N_4Samp)Cl]^{2+}$ has been prepared and subsequently crystallized as the tetrachlorozincate salt. The X-ray structure analysis confirms the pentadentate nature of the ligand and shows the thioether donor occupying one apex with four equivalent amine donors effectively occupying the equatorial plane of the molecule. The sixth coordination site is occupied by a chloro ligand. The electronic absorption and ^{13}C NMR spectra have been studied. DFT calculations have been employed to explore structural and mechanistic comparisons between $[Co(N_4Samp)Cl]^{2+}$ and an analogous pentaamine complex.

Introduction

Pentadentate chelators have been of recent interest due to their ability to give a stable coordination environment whilst allowing the binding of an additional monodentate ligand resulting in an octahedral structure about the metal cation.[1–6] The capacity of these ligands to invoke a single labile coordination site allows the possibility of their complexes to be investigated as, for example, analogues of metalloenzymes involved in substrate and O_2 activation.[5,6] Other possible applications include catalyst formation and the synthesis of coordination polymers.[4] The syntheses of a small number of ligands with a branched tetrapodal topology have been recently reported with all examples consisting of only N donors (amine, pyridine) (Chart 1).

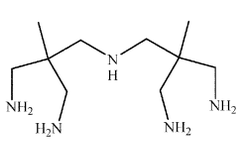

ditame

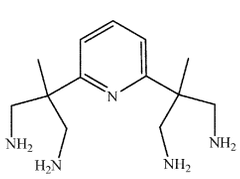

pyN_4

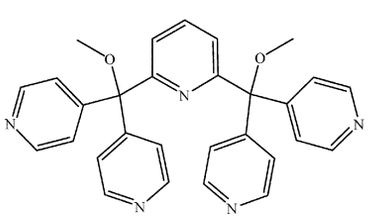

PY5

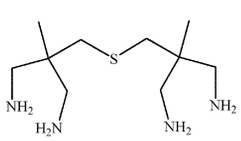

N_4Samp

Chart 1

The ligands 2,6-bis(1′,3′-diamino-2′-methylprop-2′-yl)pyridine (pyN_4) and 2,6-(bis(bis-2-pyridyl)methoxymethane)pyridine (PY5) both contain a pyridine moiety at the *hinge* position providing rigidity to the ligand structure.[1,2,5,6] The podal donor groups are all primary amines and pyridine nitrogens for pyN_4 and PY5, respectively. In the case of 2,2′-dimethyl-2,2′-iminodimethylenebis(1,3-propanediamine) (ditame), a secondary amine occupies the *hinge* site with four podal primary amine donors.[3] Whereas pyN_4 and PY5 arose from deliberate synthetic strategies, ditame was isolated as a by-product from the synthesis of ethylidynetris(methanamine) (tame).[3] For pyN_4 and ditame, the Co(III) complexes have been isolated with a chlorine atom occupying the sixth site while the analogous cobalt complex with PY5 stabilises the +II oxidation state.[1,3,5]

We now wish to report an addition to the small group of pentadentate ligands of this type, 2,6-bis(3,3-dimethyl-2,4-dioxocyclohexanyl)-4-thiaheptane (N_4Samp), structurally analogous to ditame but with a N_4S donor set where the thioether occupies the *hinge* position *trans* to the vacant sixth coordination site (Chart 1). The presence of a thioether in the donor set can potentially stabilize lower oxidation states and lower spin states of the coordinating metal ion. Our interest previously has been in the synthesis, electron transfer properties, ^{59}Co NMR and visible spectroscopy of mixed donor nitrogen–thioether cobalt(III) complexes.[7–13] We have also recently reported a potentially hexadentate N_3OS_2 ligand which is able to give pentadentate chelation in a number of forms with Co(III).[7] N_4Samp arises from a deliberate synthetic strategy utilized previously to prepare a new set of hexadentate ligands known as amplectors.[7,8]

Results and discussion

Syntheses

The synthetic strategy is described in Scheme 1. The reaction of sodium sulfide nonahydrate with 1,3-(dimethylmethylenedioxy)-2-methyl-2-(methylene-*p*-toluenesulfonyl)propane resulted in 2,6-bis(3,3-dimethyl-2,4-dioxocyclohexanyl)-4-thiaheptane, which was converted into the tetraol under dilute acid conditions. Reaction of the tetraol with toluenesulfonyl chloride and subsequent reaction of the product with potassium phthalimide in a high-boiling solvent resulted, after removal of the phthalimide with hydrazine, in the potentially pentadentate ligand 2,2,6,6-tetra(methyleneamine)-4-thiaheptane (N_4Samp). Subsequent reaction with cobalt(II) salt and oxygen resulted in, after chromatographic purification and crystallization using $NaClO_4$, the Co(III) complex as a mixed Cl^-/ClO_4^- salt. The compound was subsequently crystallized as the $ZnCl_4^{2-}$ salt, $[Co(N_4Samp)Cl](ZnCl_4)$.

DOI: 10.1039/b400710g

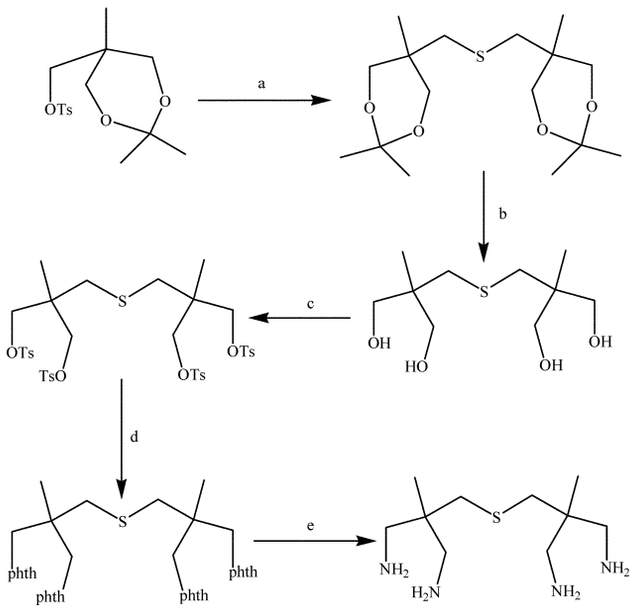

Scheme 1 Synthetic strategy for the formation of N_4Samp: (a) Na_2S (0.75 eq.)/ethanol; (b) H^+, ethanol; (c) toluenesulfonyl chloride (4.4 eq.)/pyridine; (d) potassium phthalimide (4.4 eq.)/diglyme/150 °C; (e) hydrazine hydrate (excess)/ethanol/HCl.

NMR Spectroscopy

In D_2O, the ^{13}C NMR spectrum of the complex exhibits ten resonances, suggesting the presence of two coordinated forms of N_4Samp rather than a single asymmetric complex. The intensity of five signals due to one form of the complex relative to the other five signals was found to be dependent on pH and/or Cl^- concentration (both altered with HCl). Although the two forms of the complex were detected immediately upon dissolution the equilibrium between these forms was not attained for several days after pH adjustment. The form favoured at low pH/high [Cl^-] is suggested to be the chloro species, $[Co(N_4Samp)Cl]^{2+}$, whilst under neutral conditions in the absence of added chloride, the aqua species $[Co(N_4Samp)(OD_2)]^{3+}$, becomes increasingly favoured. The ^{13}C NMR spectrum of $[Co(N_4Samp)Cl]^{2+}$ in d_6-DMSO displays five resonances indicative of a symmetric complex. Similar observations were obtained using ^1H NMR spectroscopy.

The previously reported ^{13}C spectrum of $[Co(ditame)Cl]^{2+}$ in D_2O (pD *ca.* 5) does not show any ligand exchange process at the sixth coordination site within the NMR time scale of these experiments. This suggests that the thioether donor in the Co(III) complex of N_4Samp tends to labilise the ligand at the *trans* position to this sulfur. However, this ligand lability is not found for all complexes where a chloride ligand is located *trans* to a thioether. We have recently reported two such complexes (*endo*- and *exo*-$[Co(Et(HO)N_3S_2amp)Cl]^{2+}$) where the NMR spectra in D_2O gives no indication of any ligand exchange processes occurring for both examples, within the NMR time scale of these experiments.[7]

The ^{59}Co NMR spectrum of the Co(III) complex of N_4Samp in water (pH 5.2) displays a broad resonance at δ_{Co} 7077 ppm and a weaker, broader resonance at δ_{Co} 7269 ppm. It is most likely the resonance at δ_{Co} 7077 ppm is due to $[Co(N_4Samp)Cl]^{2+}$ with a N_4SCl chromophore. For pentacyanocobaltate(III) complexes, the ^{59}Co resonance when a chloride ligand occupies the sixth site (δ_{Co} 1470 ppm) is shifted slightly downfield in comparison to the case when an ammine group is bound at the sixth position (δ_{Co} 1155 ppm).[14] This suggests that the ^{59}Co NMR resonance of the N_4SCl chromophore should be shifted slightly downfield relative to N_5S chromophores (δ_{Co} 6225–6250 ppm).[8] The second weak resonance (δ_{Co} 7269 ppm) is likely due to the presence of a small amount of $[Co(N_4Samp)(H_2O)]^{3+}$ as observed in ^{13}C and ^1H NMR studies. The substitution of a chloride ligand for a water molecule in the N_4Samp complex therefore shifts the ^{59}Co resonance ~200 ppm downfield. A downfield ^{59}Co shift of similar magnitude (370 ppm) is observed upon conversion of $[Co(CN)_5Cl]^{3+}$ to $[Co(CN)_5(H_2O)]^{2+}$.[14]

Table 1 Selected bond distances (Å) and bond angles (°) for $[Co(N_4Samp)Cl](ZnCl_4)$

Co(1)–N(1)	1.973(5)	Co(1)–N(2)	1.974(5)
Co(1)–N(3)	1.975(5)	Co(1)–N(4)	1.982(5)
Co(1)–S(1)	2.1701(17)	Co(1)–Cl(1)	2.3247(17)
N(1)–Co(1)–N(2)	86.2(2)	N(2)–Co(1)–Cl(1)	92.57(17)
N(1)–Co(1)–N(3)	98.7(2)	N(3)–Co(1)–N(4)	86.5(2)
N(1)–Co(1)–N(4)	174.7(2)	N(3)–Co(1)–S(1)	83.98(16)
N(1)–Co(1)–S(1)	84.76(16)	N(3)–Co(1)–Cl(1)	88.38(16)
N(1)–Co(1)–Cl(1)	88.63(16)	N(4)–Co(1)–S(1)	97.04(17)
N(2)–Co(1)–N(3)	175.1(2)	N(4)–Co(1)–Cl(1)	90.33(17)
N(2)–Co(1)–N(4)	88.7(3)	S(1)–Co(1)–Cl(1)	169.02(7)
N(2)–Co(1)–S(1)	95.71(17)		

Crystal structure

X-Ray analysis of crystals of the cobalt(III) complex of N_4Samp as the mixed chloride/perchloate salt indicated mixed crystal forms with possibly both aqua and chloro forms present ($[Co(N_4Samp)(H_2O)]Cl_2(ClO_4)\cdot H_2O$ and $([Co(N_4Samp)Cl]Cl(ClO_4)\cdot 2H_2O$). Subsequent crystallization from acid solution in the presence of zinc chloride resulted in the tetrachlorozincate salt. The structure of $[Co(N_4Samp)Cl](ZnCl_4)$ (Fig. 1) consists of the molecular cation and a tetrachlorozincate anion. The molecular cation has an N_4SCl donor set where the amines are coordinated to the Co(III) in a planar arrangement and the chloride ion is coordinated to the cobalt centre at the position *trans* to the thioether donor. Each of the six-membered chelate rings adopt the unsymmetrical skew-boat conformation.

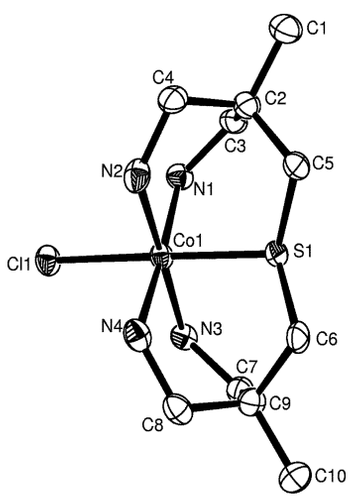

Fig. 1 ORTEP plot of the complex cation of $[Co(N_4Samp)Cl](ZnCl_4)$, giving the crystallographic atom numbering. Probability ellipsoids of 30% are shown.

The Co(III)–amine bond lengths for $[Co(N_4Samp)Cl]^{2+}$ (1.973(5), 1.974(5), 1.975(5), 1.982(5) Å) (Table 1) fall within the range of expected Co(III)–N bond lengths (1.94–2.01 Å).[15] The Co(III)–thioether bond length for $[Co(N_4Samp)Cl]^{2+}$ (2.1701(17) Å) falls below the range of Co(III)–S bond lengths for similar ligand frameworks (2.194(5)–2.275(3) Å).[16–18] The Co–Cl bond for $[Co(N_4Samp)Cl]^{2+}$ (2.3247(17) Å) is slightly longer than those reported for $[Co(pyN_4)Cl]^{2+}$ (2.2645(12) Å),[1] $[Co(ditame)Cl]^{2+}$ (2.305(4) Å)[2] and a number of other complexes where the chloride group is coordinated *trans* to an amine or pyridine nitrogen.[18–24] The elongation of the Co–Cl bond length and the shorter Co–S bond length for $[Co(N_4Samp)Cl]^{2+}$ suggest that the thioether donor has a weakening

Table 2 Comparison of calculated and experimental structural parameters (distances in Å, angles in °) for $[Co(N_4Samp)Cl]^{2+}$ and $[Co(ditame)Cl]^{2+}$ complexes

Complex	Parameter	LDA/TZP	PBE/ZORA/TZ2P	Experiment
$[Co(N_4Samp)Cl]^{2+}$	Co–Cl	2.22	2.25	2.33
	Co–S	2.14	2.18	2.17
	Co–N	1.94–1.95	1.99–2.00	1.97–1.98
	Cl–Co–S	171	171	169
	N–Co–N (*cis*)	86–98	86–98	86–99
	N–Co–N (*trans*)	174	175	175
$[Co(ditame)Cl]^{2+}$	Co–Cl	2.20	2.23	2.31
	Co–N	1.93–1.94	1.98–1.99	1.94–1.97
	Cl–Co–N (*trans*)	177	176	180
	N–Co–N (*cis*)	87–95	87–95	88–92
	N–Co–N (*trans*)	176	176	180

effect on the Co–Cl bond *trans* to itself. Similar elongation of the Co–Cl bond length in the complexes *endo*- and *exo*-$[Co(Et(HO)N_3S_2amp)]^{2+}$ is not observed (2.281(2) and 2.2771(11) Å, respectively).[7]

UV-visible spectroscopy

In DMSO the UV-visible absorption spectrum displays one transition at 17200 cm^{-1} (230 L mol^{-1} cm^{-1}), the remainder of the spectrum being obscured by an intense charge transfer band. At room temperature the Nafion film UV-visible spectrum of $[Co(N_4Samp)Cl]^{2+}$ shows the $^1A_{1g} \longrightarrow {}^1T_{1g}$ transition (19860 cm^{-1}), with the higher energy $^1A_{1g} \longrightarrow {}^1T_{2g}$ d–d transition (28340 cm^{-1}) clearly defined on a much more intense charge transfer band at 11 K. Spin forbidden transitions were not observed at 11 K. Assuming $C = 6B$, $10Dq$ was determined as 20810 cm^{-1} with $B = 645$ cm^{-1}.[11]

Calculations

DFT calculations were used to explore structural and mechanistic comparisons between $[Co(N_4Samp)Cl]^{2+}$ and the analogous pentaamine complex $[Co(ditame)Cl]^{2+}$. The results of these calculations are summarized in Tables 2 and 3, and Figs. 2–4.

Molecular structure. The molecular structures of the $[Co(N_4Samp)Cl]^{2+}$ and $[Co(ditame)Cl]^{2+}$ complexes have been fully optimized using two different computational approaches (denoted LDA/TZP and PBE/ZORA/TZ2P). Both procedures have been previously shown[8] to satisfactorily reproduce the experimental structural parameters of Co complexes similar in size and ligand environment to those investigated in this work.

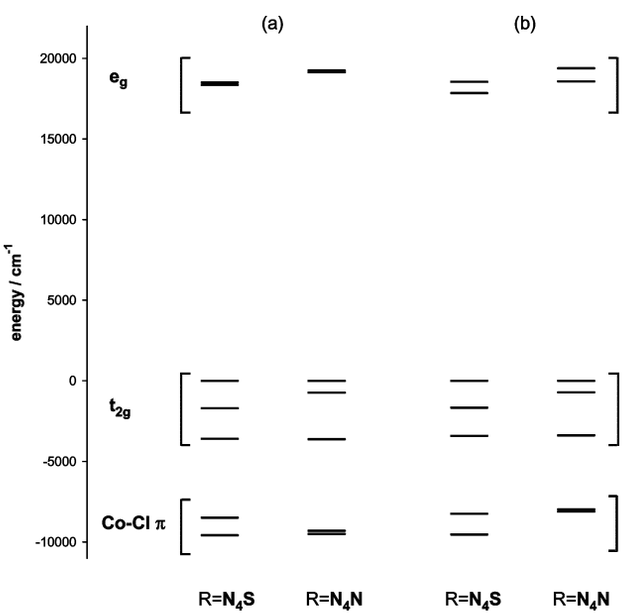

Fig. 2 Eigenvalue diagram showing some lowest-unoccupied and highest-occupied molecular orbital levels for $[Co(N_4Samp)Cl]^{2+}$ (R = N_4S) and $[Co(ditame)Cl]^{2+}$ (R = N_4N) complexes at (a) fully optimized geometry and (b) optimized geometry with experimental Co–Cl bond distance.

The calculated values for bond distances and angles involving the central Co atom are compared in Table 2 with the corresponding experimental results. All calculated parameters are in good agreement with those observed in the crystal structures, the largest (and only relatively significant) discrepancies corresponding to the Co–Cl bond length. These discrepancies are, however, likely to be caused by the fact that the computational results correspond to isolated ("gas phase") molecules, whereas the experimental parameters refer to the crystalline form of the complexes. Thus, the longer Co–Cl distances observed experimentally probably reflect the interactions of the Cl site with counterions in the solid-state environment.

The LDA/TZP and PBE/ZORA/TZ2P predictions for the Co–N distances are, respectively, slightly shorter and longer than the experimental observations, whereas the Co–S bond length (in $[Co(N_4Samp)Cl]^{2+}$) is better reproduced by the PBE/ZORA/TZ2P approach, as found in our previous work on Co complexes. Despite the aforementioned discrepancies between computational and experimental values for the Co–Cl distance, the calculations do predict a shortening of this bond in $[Co(ditame)Cl]^{2+}$ with respect to $[Co(N_4Samp)Cl]^{2+}$.

The experimental Cl–Co–S, Cl–Co–N, and N–Co–N angles are closely reproduced by the calculations, with only minor differences observed between the results obtained with the two different approaches. In particular, the computational results "correctly" predict a relatively significant deviation of the Cl–Co–S angle (in $[Co(N_4Samp)Cl]^{2+}$) from the "ideal" octahedral value of 180°.

In general, both the LDA/TZP and PBE/ZORA/TZ2P procedures can be considered to be satisfactory approaches to the computational investigation of the Co complexes studied in the present work. However, given that the latter method should (in principle) provide a more thorough description of physical and chemical phenomena, all results presented in the remaining sections are based only on PBE/ZORA/TZ2P calculations.

Electronic structure and bonding. The results of bond valency calculations on the $[Co(N_4Samp)Cl]^{2+}$ and $[Co(ditame)Cl]^{2+}$ complexes, including Mulliken charge and Mayer covalency for the Co atoms, and Mayer indexes for the Co–Cl, Co–S, and Co–N bonds, are given in Table 3.

The calculated values for the charge and covalency of the Co atoms are in accord with the differences in the ligand environment of the two complexes, as both results predict a higher degree of covalent character in the overall bonding interactions of the metal center in $[Co(N_4Samp)Cl]^{2+}$. Examination of the individual bond orders suggests that this is largely due to the greater covalency of the Co–S bond (in $[Co(N_4Samp)Cl]^{2+}$) with respect to the (corresponding) Co–N bond (in $[Co(ditame)Cl]^{2+}$).

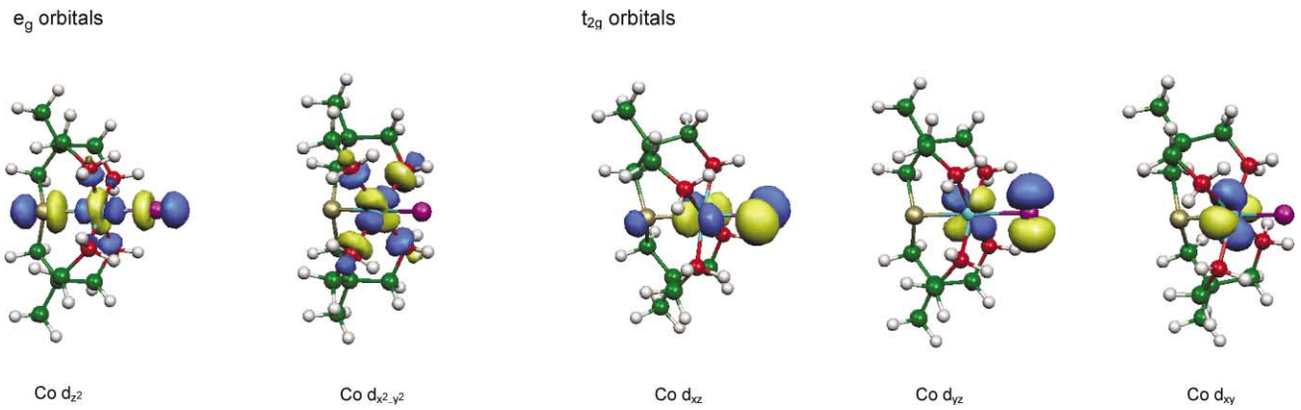

Fig. 3 Plots of the two lowest-unoccupied and three highest-occupied molecular orbitals of $[Co(N_4Samp)Cl]^{2+}$.

Table 3 Mulliken charge and covalency index for Co atoms, and Co–L (L = Cl, S, N) bond order indexes for $[Co(N_4Samp)Cl]^{2+}$ and $[Co(ditame)Cl]^{2+}$ complexes. Results are from [PBE/ZORA/TZ2P] calculations

Property	$[Co(N_4Samp)Cl]^{2+}$	$[Co(ditame)Cl]^{2+}$
Co charge	+0.29	+0.51
Co covalency	4.00	3.61
Co–Cl index	0.79	0.82
Co–S index	0.83	
Co–N index		0.57
Co–N index	0.56	0.54

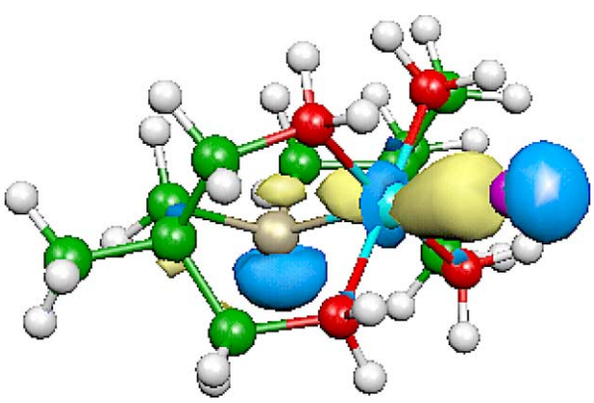

Fig. 4 Plot of a molecular orbital of $[Co(N_4Samp)Cl]^{2+}$ exhibiting S-p (lone pair)–Co-d bonding character.

The Co–Cl indexes reflect the differences in the respective bond lengths, but also suggest that the *trans* influence of the S atom in $[Co(N_4Samp)Cl]^{2+}$ does not appear to be significantly greater than that of the ("axial") N atom in $[Co(ditame)Cl]^{2+}$. This result is confirmed by the relative magnitudes of the bond dissociation energy, obtained from

$$[Co(N_4Samp)Cl]^{2+} \longrightarrow [Co(N_4Samp)]^{3+} + Cl^- \quad (1)$$

$$[Co(ditame)Cl]^{2+} \longrightarrow [Co(ditame)]^{3+} + Cl^- \quad (2)$$

The calculated values are 1282 and 1303 kJ mol^{-1}, respectively.

Eigenvalue diagrams showing some lowest-unoccupied and highest-occupied energy levels of the $[Co(N_4Samp)Cl]^{2+}$ and $[Co(ditame)Cl]^{2+}$ complexes are presented in Fig. 2. These diagrams have been constructed for both the fully optimized geometry and the partially optimized geometry where the Co–Cl distance was fixed at the experimental value. Although the actual molecular symmetry used in the calculations is C_1, it is possible to discuss the general properties of the molecular-orbital schemes by concentrating on the approximate octahedral environment of the $[CoN_4SCl]$ and $[CoN_4NCl]$ moieties.

The two lowest-unoccupied and the three highest-occupied orbitals can be associated, respectively, with the e_g and t_{2g} levels of a regular (transition metal) octahedral system. The gap between the (highest-occupied) t_{2g} and (lowest-unoccupied) e_g orbitals is predicted to be 18349 cm^{-1} for $[Co(N_4Samp)Cl]^{2+}$ and 19148 cm^{-1} for $[Co(ditame)Cl]^{2+}$. Plots of these five orbitals are given in Fig. 3 for $[Co(N_4Samp)Cl]^{2+}$. (The corresponding orbitals in $[Co(ditame)Cl]^{2+}$ are of similar character and composition.) The splitting due to the low molecular symmetry is (relatively) small in general, but nonetheless significantly larger for the t_{2g} than the e_g levels. These differences can be explained by considering the nature of the orbital interactions involved.

The five e_g and t_{2g} orbitals exhibit predominant Co d character, but while both e_g orbitals can be described as σ-antibonding interactions, the three t_{2g} orbitals can be divided into two groups with distinctly different bonding properties. The e_g σ-antibonding interactions occur between Co d_{z^2} and "axial" (Cl, S or N) ligand p-type functions, and between Co $d_{x^2-y^2}$ and "equatorial" (N) ligand p-type functions. The two highest-lying t_{2g} levels correspond to π-antibonding interactions involving primarily Co d_{xz} or d_{yz} and Cl p-type functions, whereas the third t_{2g} orbital possesses almost exclusively Co d_{xy} character with no significant contributions from the ligands, and is therefore largely nonbonding in nature.

The splitting of the e_g levels is only 50–100 cm^{-1} compared to 3600 cm^{-1} for the t_{2g} levels, but increases significantly (to 700–800 cm^{-1}) if the experimental rather than optimized Co–Cl distances are used in the calculation. This result can be related to the longer Co–Cl bond lengths observed in the crystal structures, which should weaken the Co–Cl σ-antibonding interaction involving the Co d_{z^2} orbital, thus lowering its energy with respect to the Co $d_{x^2-y^2}$ orbital.

The two levels lying below the t_{2g} orbitals can be described as possessing primarily Co d and Cl p character, although in the $[Co(N_4Samp)Cl]^{2+}$ complex some small S p contribution is also observed. These orbitals mainly involve π-bonding interactions between Co d_{xz} or d_{yz} and Cl p-type functions.

The calculations on both complexes predict distortions of the Co coordination environment from ideal octahedral geometry. Three of the "equatorial" N–Co–N angles are predicted to be slightly smaller than 90°, whereas the remaining angle has calculated values of 98° in $[Co(N_4Samp)Cl]^{2+}$ and 95° in $[Co(ditame)Cl]^{2+}$. In addition, the calculations predict greater bending of the Cl–Co–S axis in $[Co(N_4Samp)Cl]^{2+}$ (at 171°) than the Cl–Co–N axis in $[Co(ditame)Cl]^{2+}$ (at 176–177°).

A possible reason for these distortions may be found in the structural and electronic properties of the "axial" S–R_2 and NH–R_2 fragments. Some of the bending of the Cl–Co–S and Cl–Co–N axes can be related to the structural requirements and steric effects of the C–H frameworks, as a significantly greater distortion is observed for the Co–S and axial Co–N bonds than

for the Co–Cl bonds. Calculations on model $[Co(NH_3)_4(SH_2)Cl]^{2+}$ and $[Co(NH_3)_5Cl]^{2+}$ systems (where the constraints imposed by the C–H frameworks are removed) indicate that the bending of the Cl–Co–S and Cl–Co–N axes is 3–4° less than in the $[Co(N_4Samp)Cl]^{2+}$ and $[Co(ditame)Cl]^{2+}$ complexes. In $[Co(NH_3)_5Cl]^{2+}$, the *trans* Cl–Co–N angle is only slightly bent (the calculated value being 179°), but a relatively significant distortion of the Cl–Co–S angle remains in $[Co(NH_3)_4(SH_2)Cl]^{2+}$.

The larger bending of the Co–S bond in the $[Co(N_4Samp)Cl]^{2+}$ complex (and also in the model $[Co(NH_3)_4(SH_2)Cl]^{2+}$ system) is likely associated with the occurrence of interactions between S-p (lone pair) and Co-d orbitals (Fig. 4), which should favour tilting of the Co–S bond.

The distortions observed for the "equatorial" N–Co–N angles may be necessary to accommodate the structural requirements of the C–H framework in the pentadentate ligands, but it is also possible that electronic factors are involved. The spatial orientation adopted by the $S–R_2$ and $NH–R_2$ fragments implies that some of the electron density associated with the S "lone pair" in $[Co(N_4Samp)Cl]^{2+}$ or the N–H bond in $[Co(ditame)Cl]^{2+}$ lies over the plane defined by the largest "equatorial" N–Co–N angle. Repulsive interactions between the S or the N–H sites and the "equatorial" Co–N bonds may be involved in causing the value of this N–Co–N angle to increase beyond 90°.

Chloride dissociation. The dissociation of the chloro ligand as a Cl^- ion can be a central step in the mechanism of substitution reactions in species such as the $[Co(ditame)Cl]^{2+}$ complex.[3] As described in the preceding section, the chloride dissociation process – represented by eqns. (1) and (2) – in $[Co(N_4Samp)Cl]^{2+}$ and $[Co(ditame)Cl]^{2+}$ complexes is predicted to be highly endothermic if calculations correspond to "gas phase" conditions.

The thermochemical results change considerably if an approximate solvation treatment is incorporated into the computational approach. The calculated values of the dissociation energy for eqns. (1) and (2) become 71 and 81 kJ mol^{-1}, respectively, in the presence of the solvent.

Sargeson and coworkers have studied the reactivity of the $[Co(ditame)Cl]^{2+}$ complex in basic solution.[3] Under these conditions, the substitution reactions are likely to proceed *via* a conjugate base mechanism. We have also carried out calculations for the chloride dissociation process which involves the conjugate bases of the $[Co(N_4Samp)Cl]^{2+}$ and $[Co(ditame)Cl]^{2+}$ complexes.

The calculated results for the dissociation energy in the cases where deprotonation occurs at an "equatorial" (^{e}N) site are 48 kJ mol^{-1} for both

$$[Co(^eNH^-\ ^eN_3SR)Cl]^+ \longrightarrow [Co(^eNH^-\ ^eN_3SR)]^{2+} + Cl^- \quad (3)$$

and

$$[Co(^eNH^-\ ^eN_3\ ^aNR)Cl]^+ \longrightarrow [Co(^eNH^-\ ^eN_3\ ^aNR)]^{2+} + Cl^- \quad (4)$$

For the $[Co(ditame)Cl]^{2+}$ complex, deprotonation can also occur at the "axial" (^{a}N) site. In this case, the dissociation energy for

$$[Co(^aN^-\ ^eN_4R)Cl]^+ \longrightarrow [Co(^aN^-\ ^eN_4R)]^{2+} + Cl^- \quad (5)$$

is predicted to be 34 kJ mol^{-1}.

In addition to exploring the thermodynamics of chloride dissociation, we have also attempted to calculate the activation barrier for this process. However, performing a full transition state optimization, including solvation effects, is a complicated and costly computational procedure, and we have only been able to obtain results from a constrained transition state search, in which a number of single-point calculations have been carried out at an approximate transition state geometry (corresponding to Co–Cl distances between 4.50 and 5.00 Å). These calculations suggest that the activation barriers for $[Co(N_4Samp)Cl]^{2+}$ and $[Co(ditame)Cl]^{2+}$ may be similar but, due to the approximations involved, no definitive conclusions can be drawn.

Conclusion

The versatility of the amplector synthetic methodology, initially developed for the formation of hexadentate ligands, has been demonstrated by its capacity to deliberately form a pentadentate ligand with a N_4S donor set. The ligand N_4Samp is capable of forming octahedral complexes where the sixth coordination site is positioned *trans* to the thioether donor. The lability of this sixth coordination site is shown by the structural and solution properties of the complex $[Co(N_4Samp)Cl]^{2+}$.

DFT calculations were performed in order to explore some structural characteristics and the chloride dissociation properties of $[Co(N_4Samp)Cl]^{2+}$ in comparison to those of the analogous pentaamine $[Co(ditame)Cl]^{2+}$ complex. The greater tilting of the Co–S bond (in $[Co(N_4Samp)Cl]^{2+}$) with respect to the Co–N bond (in $[Co(ditame)Cl]^{2+}$) can be described as resulting from the combined effect of steric and electronic factors. The calculated Co–Cl bond dissociation properties have not been found to be substantially different. Subsequent work will investigate both the kinetics of dissociation and the range of complexes with N_4Samp formed by exchanging monodentate and bridging ligands into the sixth coordination site.

Experimental

Measurements

^1H, $^{13}C[^1H]$ and ^{13}C DEPT NMR spectra were recorded at 301 K with a Bruker AC200F 200 MHz or a Bruker AV400 400 MHz spectrometer on internal lock. Chemical shifts for the ^1H NMR spectra ($CDCl_3$, d_4-methanol and d_6-DMSO) are reported in parts per million (δ) as positive downfield of the internal reference tetramethylsilane (TMS). In D_2O, the ^{13}C chemical shifts are reported as positive downfield and negative upfield of the internal reference 1,4-dioxane.[7,8,11–13] ^{13}C NMR spectra recorded in $CDCl_3$ and d_4-methanol were referenced to the $CDCl_3$ resonance at 77 ppm and the d_4-methanol resonance at 49 ppm, respectively. In d_6-DMSO, the ^{13}C chemical shifts are reported in parts per million as positive downfield of the internal reference TMS. For ^{13}C assignments, quaternary and aromatic carbons are denoted by C_q and Ar, respectively. ^{59}Co NMR spectra (0.1 M aqueous solutions) were recorded with a Bruker AV400 400 MHz NMR spectrometer in H_2O, without lock, at 301 K ($\nu_{1/2}$ = resonance line width (Hz) at half-height). Spectra were externally referenced to $[Co(en)_3]Cl_3$ in parts per million at 7125 ppm. $K_3[Co(CN)_6]$ (0.1 M) was used as a secondary external reference at 0 ppm.

Solution UV-visible spectra were recorded with a Perkin-Elmer Lambda 40 spectrometer. Nafion films (Aldrich Nafion 117 perflourinated membrane 0.0007 in. thick) of the metal complexes as the mixed chloride perchlorate salt were prepared by placing the film in dimethylformamide solutions of the complex for 48 h. The films were removed from the solution and dried on tissue paper. In order to observe weakly absorbing bands several films were stacked on one another. UV-visible spectra of these films were recorded with a Cary 17 spectrophotometer at room temperature and at ~14 K, the low temperature spectra were obtained using a Leybold Heraeus ROK 10–300 closed cycle helium cryostat system. Where necessary, peak positions were determined using Peakfit.[25]

Calculation details

All density functional calculations reported in this article were carried out with the ADF (2002.03) program.[26–28] Functionals

based on the Volko–Wilk–Nusair (VWN)[29] form of the Local Density Approximation (LDA),[30] and on the gradient-corrected expressions proposed by Perdew, Burke and Ernzerhof (PBE)[31] were utilized. Basis sets of triple-zeta quality and one (TZP) or two (TZ2P) polarization functions, incorporating frozen cores (Co 2p, C 1s, N 1s, S 2p, Cl 2p), were employed.[26–28] Relativistic corrections were included through the ZORA approach.[32–34] The COSMO model[35] was used for the treatment of solvation effects. Atomic charges and valency indexes[36] were obtained with a program[37] designed for their calculation from the ADF output file. Graphics of molecular orbitals were generated with the MOLEKEL program.[38] Calculations on all complexes investigated utilized C_1 molecular symmetry.

Materials

1,3-(Dimethylenedioxy)-2-methyl-2-(methylene-*p*-toluenesulfonyl)propane was prepared as described previously.[39] Sodium sulfide nonahydrate was purchased from Aldrich and used without further purification.

Synthesis of N_4Samp

2,2,6-Bis(3,3-dimethyl-2,4-dioxocyclohexanyl)-4-thiaheptane. Sodium sulfide nonahydrate (57 g, 0.24 mol) was stirred in ethanol (500 cm^3) for 5 min. 1,3-(Dimethylenedioxy)-2-methyl-2-(methylene-*p*-toluenesulfonyl)propane (100 g, 0.32 mol) was added and the solution heated to reflux for 6 h. Upon cooling the solution was filtered and the solvent removed from the filtrate under reduced pressure. The residue was dissolved in $CHCl_3$ (300 cm^3) and the solution washed with water (3 × 100 cm^3). The organic layer was separated, dried over Na_2SO_4, filtered and the solvent removed under reduced pressure to yield a yellow oil (42.8 g, 56%). ^{13}C NMR ($CDCl_3$): δ_C 19.1 ($–CH_3$); 20.8, 26.4 ($CH_3–C_qO$); 34.2 (C_q); 40.5 ($–CH_2–S$); 67.9 ($–CH_2–O$); 97.7 ($C_q–O$). ^{1}H NMR ($CDCl_3$): δ_H 0.89 ($–CH_3$, s); 1.39, 1.41 ($CH_3–C_qO$, s); 2.78 ($–CH_2–S$, s); 3.63 ($–CH_2–O$, dd).

2,2,6,6-Tetra(hydroxymethyl)-4-thiaheptane. 2,6-Bis(3,3-dimethyl-2,4-dioxocyclohexanyl)-4-thiaheptane (42.8 g) was dissolved in ethanol (400 cm^3) and heated at reflux. Concentrated HCl (20 cm^3) was added and the reflux continued for 10 min. Upon cooling, the solvent was removed under reduced pressure to yield a brown oil (36.4 g, quantitative). ^{13}C NMR (d_4-methanol): δ_C 18.8 ($–CH_3$); 40.3 ($–CH_2–S$); 42.3 (C_q); 66.9 ($–CH_2–O$). ^{1}H NMR (d_4-methanol): δ_H 0.92 ($–CH_3$, s); 2.60 ($–CH_2–S$, s); 3.47 ($–CH_2–O$, dd).

2,2,6.6-Tetra(methylene-*p*-toluenesulfonyl)-4-thiaheptane. 2,2,6,6-Tetra(hydroxymethyl)-4-thiaheptane (36.4 g) was dissolved in dry pyridine (200 cm^3) and the solution cooled in an ice-bath. To the stirred solution, *p*-toluenesulfonyl chloride (128 g) dissolved in dry pyridine (400 cm^3) was added dropwise over 2 h. The reaction mixture was allowed to warm to room temperature and stirring maintained for 48 h. The mixture was poured into a solution of concentrated HCl (275 cm^3), water (350 cm^3) and methanol (700 cm^3) to precipitate an off-white solid which was extracted with $CHCl_3$ (3 × 300 cm^3). The extracts were combined and washed with water (2 × 300 cm^3). The $CHCl_3$ solution was separated, dried over Na_2SO_4, filtered and the solvent removed under reduced pressure to yield a golden oil (101.3 g, 78%). ^{13}C NMR ($CDCl_3$): δ_C 18.0 ($–CH_3$); 21.6 ($–CH_3$ (tosylate)); 38.7 ($–CH_2–S$); 39.7 (C_q); 71.2 ($–CH_2–O$); 127.8, 130.0, 132.0, 145.2 (Ar (tosylate)). ^{1}H NMR ($CDCl_3$): δ_H 0.85 ($–CH_3$, s); 2.36 ($–CH_2–S$, s); 2.45 ($–CH_3$ (tosylate), s); 3.77 ($–CH_2–O$, dd); 7.49 (Ar–H (tosylate), dd).

2,2,6,6-Tetra(methylenephthalimido)-4-thiaheptane. 2,2,6.6-Tetra(methylene-*p*-toluenesulfonyl)-4-thiaheptane (39.6 g) and potassium phthalimide (37.8 g) were suspended in diethylene glycol dimethyl ether (150 cm^3) and the mixture heated at 150 °C for 18 h. The cooled solution was poured into water (600 cm^3) to precipitate a brown oil. The mixture was allowed to stand for 24 h and filtered to yield a pale brown solid. The solid was dissolved in $CHCl_3$ (600 cm^3), dried over Na_2SO_4, filtered and the solvent removed under reduced pressure to give a pale brown oil (35.8 g). The product was used without further purification.

2,2,6,6-Tetra(methyleneamine)-4-thiaheptane (N_4Samp). 2,2,6,6-Tetra(methylenephthalimido)-4-thiaheptane (19.1 g) was suspended in ethanol (250 cm^3) and heated at reflux. Hydrazine monohydrate (51 cm^3, 98%) was added to the refluxing solution. Over a period of 5 min the solution became clear then a dense white precipitate formed. The reflux was maintained for 2 h. The solution was cooled in an ice bath and concentrated HCl (40 cm^3) added dropwise. The mixture was heated at reflux for a further 40 min, cooled and the solvent removed under reduced pressure. The residue was dissolved in water (200 cm^3) and the solution filtered. The filtrate was made strongly alkaline with KOH and the product extracted with $CHCl_3$ (3 × 100 cm^3). The $CHCl_3$ extracts were combined, dried over Na_2SO_4, filtered and the solvent removed under reduced pressure to yield a brown oil (4.1 g). The product was used without further purification.

CAUTION: Although the perchlorate salts described in this work do not appear to be sensitive to shock or heat these materials, like all perchlorates, should be treated with caution.

[Co(N_4Samp)Cl]($ZnCl_4$). Cobaltous nitrate hexahydrate (19.5 g) in methanol (500 cm^3) was added dropwise to the stirred mixture of ligand (19.5 g) dissolved in methanol (400 cm^3). A stream of air was bubbled through the ligand solution for the duration of the addition and continued for a further 4 h. The solvent was removed under reduced pressure, the residue dissolved in water and the solution filtered. The filtrate was diluted to 2 L and loaded on Dowex cation exchange resin (50W × 2 (200–400 mesh) H^+ form). The column was washed with water and 1 M HCl to elute minor products. The major pink/purple band was eluted with 2 M HCl. The solvent was removed from pink/purple eluent under reduced pressure to give an impure pink residue. The residue was dissolved in a minimum volume of aqueous $NaClO_4$ and pink needle like crystals formed overnight (0.3 g, 0.7%). Analysis of these crystals indicated a mixed chloride/perchlorate salt of the complex had formed. Analysis. Calc. for $C_{10}H_{26}N_4SCoCl_2(ClO_4)\cdot 2H_2O$: C, 24.03; H, 6.05; N, 11.21. Found: C, 24.16; H, 5.74; N, 11.10%. The crystals were dissolved in water, acidified with HCl, and $ZnCl_2$ was added to give an immediate purple precipitate. The precipitate was filtered and dissolved in a minimum of water with heating. Purple crystals were grown from the aqueous solution by vapour diffusion with ethanol. Analysis. Calc. for $[C_{10}H_{26}N_4SClCo]ZnCl_4$: C, 22.41; H, 4.89; N, 10.46. Found: C, 22.22; H, 4.95; N, 10.21%. UV-visible spectrum [λ_{max} /nm (ε_{max}/L mol^{-1} cm^{-1}) in DMSO]: 580 (230). ^{13}C NMR (d_6-DMSO): δ_C 24.1 ($–CH_3$); 33.6 ($–CH_2–S$); 40.2 (C_q); 44.3, 45.0 ($–CH_2–N$). ^{1}H NMR (d_6-DMSO): δ_H 0.93 ($–CH_3$, s); 2.75 ($–CH_2–S$, dd); 4.7, 6.0 ($–NH_2$, dd). ^{59}Co NMR (H_2O, pH 5.2): δ_{Co} 7077 ($\nu_{1/2}$ = 5350 Hz). ESI-MS: Calc. for [Co(N_4Samp)^{35}Cl]$^{2+}$ − H^+, *m*/*z* 327. Found, *m*/*z* 327 (91%). Calc. for [Co(N_4Samp)]$^{3+}$ − $2H^+$, *m*/*z* 291. Found, *m*/*z* 291 (100%).

Crystallography

Data collection and processing. For diffractometry the crystal was mounted onto glass fibres with Supa Glue. Lattice parameters were determined by least squares fits to the setting parameters of 25 independent reflections, measured and refined with an Enraf-Nonius CAD4 diffractometer using graphite-monochromated Mo-Kα radiation (λ = 0.71073 Å). Formula: $C_{10}H_{26}Cl_5CoN_4SZn$, M = 535.96, monoclinic, space group $P2_1/c$, T = 293(2) K, a = 7.861(2), b = 15.432(2), c = 16.856(2) Å, β =

98.64(2)°, $V = 2021.6(6)$ Å^3, $Z = 4$, $\mu = 27.70$ cm^{-1}, 3550 unique data, $R_{int} = 0.0488$, $R(F_o) = 0.0510$, $R_w = 0.0869$.

Structure analysis and refinement. The structure was solved by heavy-atom methods (direct methods) and refined using full-matrix least squares on F^2. Programs used were SHELXS-86 [40] for solution, SHELXL-97 [41] for refinement and ORTEP-3 for Windows [42] for plotting. The geometry of the molecule is shown in Fig. 1 together with the atomic numbering scheme. Selected bond lengths and bond angles are given in Table 1.

CCDC reference number 228914.

See http://www.rsc.org/suppdata/dt/b4/b400710g/ for crystallographic data in CIF or other electronic format.

References

1 A. Grohmann and F. Knoch, *Inorg. Chem.*, 1996, **35**, 7932.
2 J. P. López, F. W. Heinemann, R. Prakash, B. A. Hess, O. Horner, C. Jeandet, J.-L. Oddou, J.-M. Latour and A. Grohmann, *Chem. Eur. J.*, 2002, **8**, 5709.
3 B. Fabius, R. J. Geue, R. G. Hazell, W. G. Jackson, F. K. Larsen, C. J. Qin and A. M. Sargeson, *J. Chem. Soc., Dalton Trans.*, 1999, 3961.
4 K. Hegetschweiler, O. Maas, A. Zimmer, R. J. Geue, A. M. Sargeson, J. Harmer, A. Schweiger, I. Buder, G. Schwitzgebel, V. Reiland and W. Frank, *Eur. J. Inorg. Chem.*, 2002, **41**, 4633.
5 R. J. M. K. Gebbink, R. T. Jonas, C. R. Goldsmith and T. D. P. Stack, *Inorg. Chem.*, 2002, **41**, 4633.
6 C. R. Goldsmith, R. T. Jonas, A. P. Cole and T. D. P. Stack, *Inorg. Chem.*, 2002, **41**, 4642.
7 C. A. Sharrad, S. R. Lüthi and L. R Gahan, *Dalton Trans.*, 2003, 3693.
8 C. A. Sharrad, G. E. Cavigliasso, R. Stranger and L. R. Gahan, *Dalton Trans.*, 2004, 767.
9 T. M. Donlevy, L. R. Gahan, T. W. Hambley, K. L. McMahon and R. Stranger, *Aust. J. Chem.*, 1993, **46**, 1799.
10 L. R. Gahan, T. W. Hambley, A. M. Sargeson and M. R. Snow, *Inorg. Chem.*, 1982, **21**, 2699.
11 L. R. Gahan, T. M. Donlevy and T. W. Hambley, *Inorg. Chem.*, 1990, **29**, 1451.
12 T. M. Donlevy, L. R. Gahan, T. W. Hambley and R. Stranger, *Inorg. Chem.*, 1992, **31**, 4376.
13 J. I. Bruce, L. R. Gahan, T. W. Hambley and R. Stranger, *Inorg. Chem.*, 1993, **32**, 5997.
14 T. Fujihara and S. Kaizaki, *J. Chem. Soc., Dalton Trans.*, 1993, 1275.
15 P. Hendry and A. Ludi, *Adv. Inorg. Chem.*, 1990, **35**, 117.
16 P. Osvath, A. M. Sargeson, A. McAuley, R. E. Mendelez, S. Subramanian, M. J. Zaworotko and L. Broge, *Inorg. Chem.*, 1999, **38**, 3634.
17 G. J. Grant, S. S. Shoup, C. E. Hadden and D. G. VanDerveer, *Inorg. Chim. Acta.*, 1998, **274**, 192.
18 G. Wei, C. C. Allen, T. W. Hambley, G. A. Lawrance and M. Maeder, *Inorg. Chim. Acta*, 1997, **261**, 197.
19 G. A. Lawrance, M. Martinez, B. W. Skelton and A. H. White, *J. Chem. Soc., Dalton Trans.*, 1992, 1649.
20 J. A. Stanko and I. C. Paul, *Inorg. Chem.*, 1967, **6**, 487.
21 G. Bombieri, E. Forsellini, A. D. Pra and M. L. Tobe, *Inorg. Chim. Acta*, 1980, **40**, 71.
22 G. Bombieri, E. Forsellini, A. D. Pra and M. L. Tobe, *Inorg. Chim. Acta*, 1981, **51**, 177.
23 G. Bombieri, E. Forsellini, A. D. Pra, M. L. Tobe and R. Henderson, *Gazz. Chim. Ital.*, 1979, **109**, 207.
24 J. L. Flückiger, C. W. Schläpfer and C. Couldwell, *Inorg. Chem.*, 1980, **19**, 2493.
25 PeakFit, Version 4, AISN Software Inc., 1991-1995.
26 ADF2002.03, SCM, Theoretical Chemistry, Vrije Universiteit, Amsterdam, The Netherlands (http://www.scm.com).
27 C. Fonseca Guerra, J. G. Snijders, G. te Velde and E. J. Baerends, *Theor. Chem. Acc.*, 1998, **99**, 391.
28 G. te Velde, F. M. Bickelhaupt, S. J. A. van Gisbergen, C. Fonseca Guerra, E. J. Baerends, J. G. Snijders and T. Ziegler, *J. Comput. Chem.*, 2001, **22**, 931.
29 S. H. Vosko, L. Wilk and M. Nusair, *Can. J. Phys.*, 1980, **58**, 1200.
30 W. Kohn and L. J. Sham, *Phys. Rev.*, 1965, **140**, A1133.
31 J. P. Perdew, K. Burke and M. Ernzerhof, *Phys. Rev. Lett.*, 1996, **77**, 3865.
32 E. van Lenthe, E. J. Baerends and J. G. Snijders, *J. Chem. Phys.*, 1993, **99**, 4597.
33 E. van Lenthe, E. J. Baerends and J. G. Snijders, *J. Chem. Phys.*, 1994, **101**, 9783.
34 E. van Lenthe, A. E. Ehlers and E. J. Baerends, *J. Chem. Phys.*, 1999, **110**, 8943.
35 C. C. Pye and T. Ziegler, *Theor. Chem. Acc.*, 1999, **101**, 396.
36 I. Mayer, *Chem. Phys. Lett.*, 1983, **97**, 270.
37 A. J. Bridgeman and C. J. Empson, MAYER, University of Hull, England, 2002.
38 S. Portmann and H. P. Lüthi, *Chimia*, 2000, **54**, 766.
39 V. W. Gash, *J. Org. Chem.*, 1972, **37**, 2197.
40 A. Altomare, G. Cascorano, C. Giacovazzo and A. Gualardi, *J. Appl. Crystallogr.*, 1993, **26**, 343.
41 G. M. Sheldrick, SHELXL-97, A program for crystal structure determination, University of Göttingen, 1997.
42 L. J. Farrugia, *J. Appl. Crystallogr.*, 1997, **30**, 565.